



CHALMERS

Chalmers Publication Library

Thermal depth profiling of materials for defect detection using hot disk technique

This document has been downloaded from Chalmers Publication Library (CPL). It is the author's version of a work that was accepted for publication in:

AIP Advances (ISSN: 2158-3226)

Citation for the published paper:

Mihiretie, B. ; Cederkrantz, D. ; Sundin, M. et al. (2016) "Thermal depth profiling of materials for defect detection using hot disk technique". AIP Advances, vol. 6(8), pp. artikel nr 085217.

<http://dx.doi.org/10.1063/1.4961879>

Downloaded from: <http://publications.lib.chalmers.se/publication/240738>

Notice: Changes introduced as a result of publishing processes such as copy-editing and formatting may not be reflected in this document. For a definitive version of this work, please refer to the published source. Please note that access to the published version might require a subscription.

Chalmers Publication Library (CPL) offers the possibility of retrieving research publications produced at Chalmers University of Technology. It covers all types of publications: articles, dissertations, licentiate theses, masters theses, conference papers, reports etc. Since 2006 it is the official tool for Chalmers official publication statistics. To ensure that Chalmers research results are disseminated as widely as possible, an Open Access Policy has been adopted. The CPL service is administrated and maintained by Chalmers Library.

(article starts on next page)



Thermal depth profiling of materials for defect detection using hot disk technique

B. M. Mihiretie, D. Cederkrantz, M. Sundin, A. Rosén, H. Otterberg, Å. Hinton, B. Berg, and M. Karlsteen

Citation: *AIP Advances* **6**, 085217 (2016); doi: 10.1063/1.4961879

View online: <http://dx.doi.org/10.1063/1.4961879>

View Table of Contents: <http://scitation.aip.org/content/aip/journal/adva/6/8?ver=pdfcov>

Published by the *AIP Publishing*

Articles you may be interested in

[Thermal conductivity versus depth profiling of inhomogeneous materials using the hot disk technique](#)

Rev. Sci. Instrum. **87**, 074901 (2016); 10.1063/1.4954972

[Response to "Comment on 'Measurement of thermal diffusivity at high-pressure using a transient heating technique'" \[Appl. Phys. Lett.95, 096101 \(2009\)\]](#)

Appl. Phys. Lett. **95**, 096102 (2009); 10.1063/1.3216045

[Reconstruction of depth profiles of thermal conductivity of case hardened steels using a three-dimensional photothermal technique](#)

J. Appl. Phys. **104**, 113518 (2008); 10.1063/1.3035831

[Parameter estimations for measurements of thermal transport properties with the hot disk thermal constants analyzer](#)

Rev. Sci. Instrum. **71**, 2452 (2000); 10.1063/1.1150635

[Thermal wave depth profile of subsurface defect in opaque solids using mirage effect \(PDS\) \[Revisited\]](#)

AIP Conf. Proc. **463**, 164 (1999); 10.1063/1.58034

The advertisement features a blue and orange background with a molecular structure graphic. On the left is a thumbnail of the journal cover for 'AIP Applied Physics Reviews'. The main text reads 'NEW Special Topic Sections' in large white letters. Below this, it says 'NOW ONLINE' in orange, followed by 'Lithium Niobate Properties and Applications: Reviews of Emerging Trends' in white. The AIP Applied Physics Reviews logo is in the bottom right corner.

NEW Special Topic Sections

NOW ONLINE
Lithium Niobate Properties and Applications:
Reviews of Emerging Trends

AIP Applied Physics Reviews

Thermal depth profiling of materials for defect detection using hot disk technique

B. M. Mihiretie,¹ D. Cederkrantz,^{2,a} M. Sundin,³ A. Rosén,³ H. Otterberg,²
Å. Hinton,⁴ B. Berg,⁴ and M. Karlsteen^{1,b}

¹Department of Physics, Chalmers University of Technology, SE-41296 Gothenburg, Sweden

²Hot Disk AB, SE-41288 Gothenburg, Sweden

³Department of Physics, Gothenburg University, SE-41296 Gothenburg, Sweden

⁴Ale Animal Clinic, SE-449 34 Ale, Sweden

(Received 5 July 2016; accepted 11 August 2016; published online 24 August 2016)

A novel application of the hot disk transient plane source technique is described. The new application yields the thermal conductivity of materials as a function of the thermal penetration depth which opens up opportunities in nondestructive testing of inhomogeneous materials. The system uses the hot disk sensor placed on the material surface to create a time varying temperature field. The thermal conductivity is then deduced from temperature evolution of the sensor, whereas the probing depth (the distance the heat front advanced away from the source) is related to the product of measurement time and thermal diffusivity. The presence of inhomogeneity in the structure is manifested in thermal conductivity versus probing depth plot. Such a plot for homogeneous materials provides fairly constant value. The deviation from the homogeneous curve caused by defects in the structure is used for inhomogeneity detection. The size and location of the defect in the structure determines the sensitivity and possibility of detection. In addition, a complementary finite element numerical simulation through COMSOL Multiphysics is employed to solve the heat transfer equation. Temperature field profile of a model material is obtained from these simulations. The average rise in temperature of the heat source is calculated and used to demonstrate the effect of the presence of inhomogeneity in the system. © 2016 Author(s). All article content, except where otherwise noted, is licensed under a Creative Commons Attribution (CC BY) license (<http://creativecommons.org/licenses/by/4.0/>). [<http://dx.doi.org/10.1063/1.4961879>]

I. INTRODUCTION

The conventional nondestructive techniques for material inspection include radiography, ultrasonics, liquid penetrant, eddy current, magnetic and thermal methods. Thermal methods work on the principle that two different materials provide distinct thermal response while interacting with thermal signal.¹⁻³ Thermal imaging is a powerful tool for nondestructive characterization of materials. It has a wide range of practical applications in industries such as in aerospace. It comprises of various imaging schemes such as thermography (IR imaging), thermoacoustic imaging, mirage effect etc.⁴⁻⁶ The article reports a new thermal method of inhomogeneous detection by monitoring the temperature change in an external heat source and deducing the thermal conductivity of the material as a function of distance from the source.

The experimental techniques for thermal conductivity measurement are categorized in two broad groups: steady-state and transient techniques.⁷ The steady-state method requires longer measurement time and large sample dimension whereas the transient technique enables fast measurement. Examples of the latter method includes transient: hot wire,⁸ hot strip⁹ and plane source techniques.¹⁰ The

^adaniel.cederkrantz@hotdisk.se

^bmagnus.karlsteen@chalmers.se



transient plane source method, which is called Hot Disk, is a primary tool for characterizing thermal transport properties of materials. It has been found to be an excellent method to determine thermal transport properties of solids, liquids, powders, pastes and laminate.¹¹ The hot disk technique adheres to an ISO standard for testing thermal transport properties of homogeneous materials.¹² There is however an interest to extend the technique to study inhomogeneous materials. Sizov *et al.*¹³ developed an approximation scheme for determining the thermal conductivity of inhomogeneous materials based on the original hot disk method, i.e temperature evolution of the sensor (the transient curve) is fitted to the theoretical model (eqn. (1)) from which the thermal conductivity is obtained. The new iteration scheme considers short time windows of the transient curve to estimate the thermal conductivity of depth position. They demonstrated the method using few examples.

This article shows the possibility of inhomogeneity detection in a material through thermal conductivity variation which is not present in a homogeneous system. This method has possible applications in quality control such as testing sample homogeneity and sample reproducibility in characterizing component gradient etc.

The study focuses in evaluating the hot disk method as a tool to analyze inhomogeneity and defects in a sample. Detail polymer samples have been fabricated using 3D printing. The printed samples have been prepared with voids of different sizes and positions in the matrix. These samples have then been studied experimentally using the hot disk method. The commercially available COMSOL Multiphysics software have been employed to numerically solve the heat transfer in the samples. The simulation results have been used to complement the experimental data.

Sec. II of this article briefly describes the theory of hot disk technique. In sec. III, we present the experimental method which addresses details of the experimental setup and description of the sample materials. The computational procedure is presented in sec. IV. Sec. V consists of result and discussion. The conclusion is presented in sec. VI.

II. THEORY

The fundamental hot disk technique is based on using a double spiral of conducting metal simultaneously as continuous heat source and sensor. The spiral generates heat which diffuses into the sample. Solving the heat conduction equation for the spiral geometry provides a relation between the change in the sensor temperature and the thermal conductivity of the material.

$$\overline{\Delta T}(\tau) = \frac{P_o}{\pi^{\frac{3}{2}} a K} D(\tau) \quad (1)$$

For $\tau = \frac{\sqrt{\kappa t}}{a}$, $K = \kappa \rho c$, κ is thermal diffusivity, t is the test time, a is the radius of the largest ring in the sensor, P_o is output power, K is thermal conductivity, ρc is the volumetric specific heat of the material and $D(\tau)$ is a complex function of time.^{7,11}

The sensor temperature increase is acquired by monitoring the change in resistance during heating. The average change in temperature over the sensor is related to its electrical resistance:

$$R = R_o [1 + \alpha \overline{\Delta T}(t)], \quad (2)$$

Where R is the total resistance at time t , R_o is initial resistance, α is the temperature coefficient of resistance of the spiral and $\overline{\Delta T}(t)$ is the average change in sensor temperature.^{7,11}

The temperature of the sensor increases with time. Eqn. (1) shows that this increase in temperature depends on the thermal property of the surrounding material. The temperature evolution of the sensor versus time is fitted to eqn. (1) to yield the thermal conductivity of the homogeneous material. But in the case of inhomogeneous material the problem gets more complicated, as there is no known mathematical model to fit the data. However, a unique feature of the hot disk method is that the thermal penetration depth can be determined as a function of the measurement time. This is described by the following relationships:

$$d_p = 2\sqrt{\kappa t}, \quad (3)$$

where d_p represents the thermal depth of probing.

Thus, eqn. (3) is exploited to extend the mathematical model to approximate the thermal conductivity of inhomogeneous materials.¹³ This is achieved by considering smaller time intervals in the transient curve, i.e instead of fitting the entire transient curve once, the fitting is limited to smaller time windows, $[t_i, t_{i+N}]$, where N is the number of points in the new limited time window. This results in local thermal conductivity and diffusivity values. Sliding the limited time window across the entire time range estimate the thermal conductivity of the sample along the probing depth which is calculated from the average estimated thermal diffusivity. The challenge of fitting the model to the small time window is overcome by an *a-priori*-known volumetric specific heat capacity of the sample.

III. EXPERIMENTAL METHOD

Experimental and numerical technique are applied to demonstrate the capability and investigate the limitation of the method.

A. Experimental Setup

The experiments employed in this study incorporate a Hot Disk TPS 2500 S thermal analyzer, four hot disk sensors with different radius, hot disk data analysis software and four sample materials, fig. 1.

In the experiment, the top side of the sensor is insulated with EPS (expanded polystyrene) to direct the heat flow into the sample material. Load is applied on the top of the insulating material in order to get good thermal contact between sensor and sample. The measurement proceeds by selecting appropriate heating power, measurement time and sensor type. The sensor radius is determined by sample thickness as larger radius sensors can probe deeper. Hot disk sensors with radii of 0.526, 2.001, 3.18 and 9.868 mm are used. The heating power is affected by the thermal property of the material and sensor radius. The ideal heating power should be able to raise the temperature of the sensor to few Kelvin, typically 2 - 5 K. Measurement time should be long enough so that the heat wave reaches the desired area but short enough not to reach the rear sample surface. To achieve reproducibility, it is important to let the sample temperature stabilize between each measurements.

B. Sample Design

Four groups of sample materials are prepared from polymers and Pyrex glass. Each of the samples is designed to investigate a particular purpose. In doing so different size and shape defects are introduced into the samples.

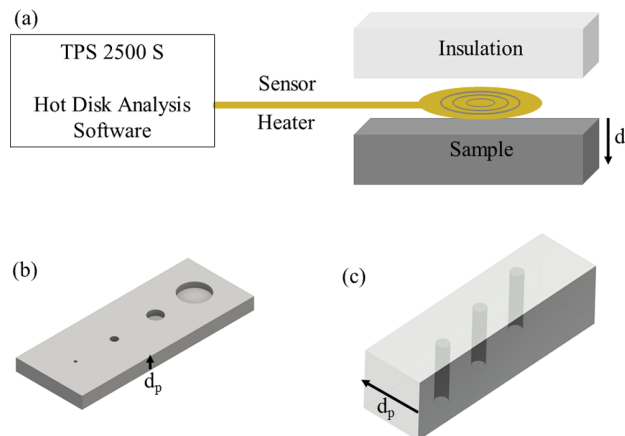


FIG. 1. (a) Simplified experimental sketch. The direction of heat flow from the sensor to the sample thickness is indicated by the arrow, d_p . (b) Sketch of sample II, the sensor is placed on the opposite side of the void. (c) Sketch of sample III, the sensor is placed on the front side of the material.

Sample I: Consists of samples that are made by 3D printing of ABS (Acrylonitrile Butadiene Styrene) and PLA (Polylactic acid) polymers. Each sample has a surface area of $50 \times 50 \text{ mm}^2$ and a thickness of 10 mm. In a typical experiment the sensor is placed on the center of the surface area and the thermal conductivity perpendicular to the plane is investigated. This sample shows the thermal conductivity of a homogeneous material, fig. 3.

Sample II: PVC (Polyvinyl chloride) plastic sheet with four cylindrical defects. The sample has a surface area of $130 \times 50 \text{ mm}^2$ and thickness of 9 mm. The four defects have radii of 10, 5, 2.5 and 1 mm, fig. 1(b), and they are all placed at a depth of ~ 4.5 mm from the surface. Measurements on this sample compares the effect of defect size, fig. 4.

Sample III: Pyrex glass with dimensions $70 \times 20 \times 20 \text{ mm}^3$. Three defects with a diameter of 2 mm are prepared in the sample at a distance of 2.5, 3.5 and 4.5 mm from one side, see fig. 1(c). Experiments performed on this sample test the detection sensitivity as a function of distance between sensor and defect, fig. 5.

Sample IV: Consist of 3D printed polymer prism with a void in the center. The prism is a hexagon with a triangular void ($20 \times 20 \times 3 \text{ mm}^3$) located inside. Fig. 6 shows measurement from sample IV.

Experiments on sample I and IV used sensor with radius of 9.868 mm. Experiments on sample III used a sensor of radius 3.18 mm whereas experiments performed on sample II requires the use of multiple sensors for comparison, table I.

IV. COMPUTATIONAL PROCEDURE

The present model considers a polymer material exposed to a series of very thin concentric heating elements on its surface. The model is generated using COMSOL Multiphysics V. 5. 2 software. The aim of the simulation is to develop transient heat conduction model and demonstrate the role of inhomogeneity on the transient curve. The governing equation that describes transient heat transfer in solids can be expressed as follows:¹⁴

$$\rho c \cdot \frac{\partial T(r,t)}{\partial t} = \nabla \cdot (K \cdot \nabla T(r,t)) + Q \quad (4)$$

where Q is the heat source per unit volume and r is position vector.

The validation of COMSOL's heat transfer modules is documented in different studies.¹⁵⁻¹⁷ A typical COMSOL simulation comprises of choosing the physics and solver type, defining geometry and materials, applying appropriate boundary conditions and meshes.

The following boundary conditions are considered:

- Extremities of the model are insulated.

$$\mathbf{n} \cdot \mathbf{q} = 0 \quad (5)$$

where \mathbf{n} is normal vector and \mathbf{q} is the heat flux by conduction.

- Thermal contact boundary condition is set between the heat source and the sample. It determines the heat flux across the surface.
- The initial values of the temperature for all domains were set to be at room temperature (293.15 K).
- The heat source is defined using a thin concentric elements with over all heat transfer rate.
- Heat loss due to convection is considered at the boundaries subjected to air (void region).
- Physics controlled mesh of user defined element size is adapted for all the domains. The meshing was refined till the solutions are independent of the meshing size.

An example of a meshed model is shown in fig. 2. The figure is the model material for sample II. The double spiral heat source (nickel wire) of radius 10 mm is placed opposite to the largest defect. The temperature increase over time of all the domains due to the constant heat from the source is computed using time dependent solver. Using the above conditions, eqn. (4) is solved for the dependent variable temperature and the results are presented in fig. 8 - 10.

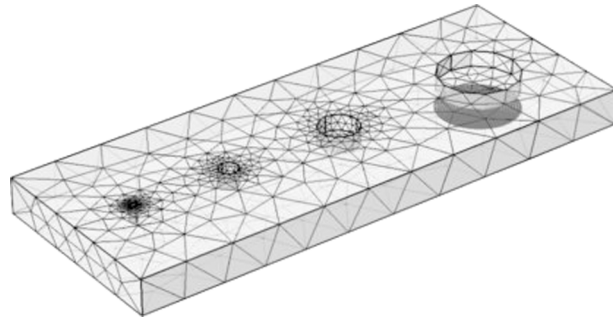


FIG. 2. Meshed geometry. The dimension and property of the model is kept similar to sample II.

V. RESULT AND DISCUSSION

A. Experimental observation

Fig. 3 - 6 show the thermal conductivity measurements along the material depth. Each of the four figures are obtained from measurements carried out on the sample I - IV respectively.

Fig. 3 represents the property of a homogeneous material. The constant thermal conductivity along the depth as demonstrated in the figure confirms the homogeneity of materials in sample I. Each curve in the figure is the average value of multiple measurements. The initial points recorded are excluded due to boundary effects of sensor and contact resistance. Thus, during calculation of thermal conductivity it is necessary to correctly select a suitable data range. The variation in magnitude between curves in fig. 3 comes from the different polymers used to print the sample and the particular printing setting used.

Fig. 4 - 7 address the experimental results that demonstrate the capability and limitation of the method in inhomogeneity detection. We characterize detection as the observed change in magnitude of thermal conductivity as a function of thermal penetration depth.

Fig. 4 demonstrates the effect of the presence of inhomogeneity in the structure. It contains measurements performed on sample II, fig. 1(b). The lower two curves (solid line and dash-dot line) show a clear presence of a different material with different thermal conductivity. The solid line and dash-dot line represent measurements performed on the sample with defect diameter of 20 and

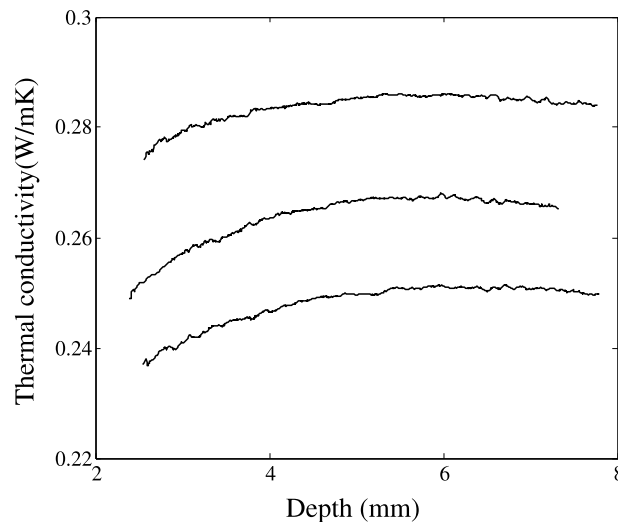


FIG. 3. Thermal conductivity of 3D printed polymers (sample I) along the structure depth. The top curve is from PLA whereas the lower two curves are from ABS polymers. A sensor of radius 9.868 mm, power of 100 mW and measurement time of 80 s are used in these experiments.

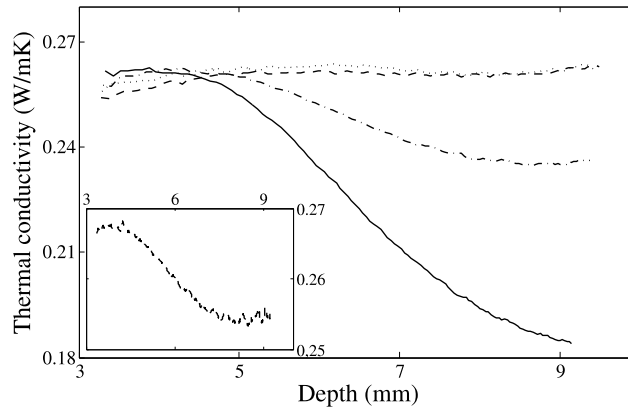


FIG. 4. Thermal conductivity plot of sample II. The Solid line, dash-dot line, dashed line and dotted lines represent measured value at 20, 10, 5, and 2 mm diameter defects, respectively, using 9.868 mm radius sensor. The inset is thermal conductivity of 5 mm diameter defect measured using 3.18 mm radius sensor.

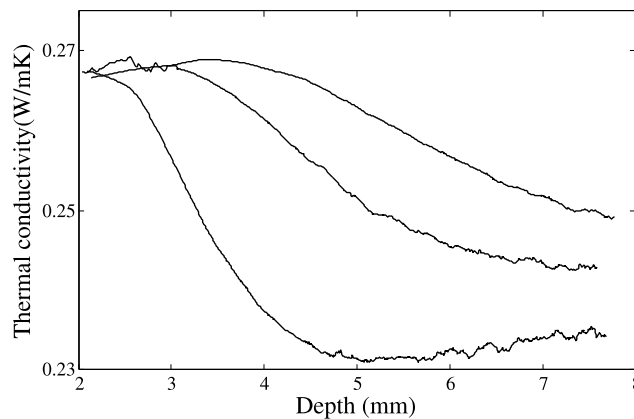


FIG. 5. Comparison of three defect detections at different location. The lower, middle and top curves represent defects located at 2.5, 3.5 and 4.5 mm away from the sensor, respectively.

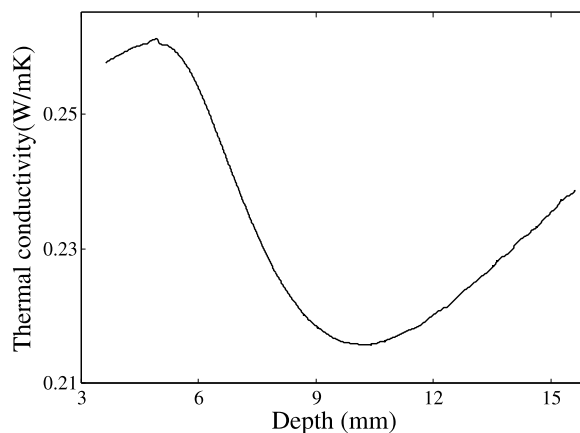


FIG. 6. Thermal conductivity of a 3D printed polymer with a void inside.

10 mm respectively. The value starts to fall down starting from ~ 4.5 mm inside the material. The detection is more visible in the case of largest defect. Whereas, the dotted and dashed line show constant value implying that detection is not possible. These lines represent the defect with diameter of 5 mm (dashed line) and 2 mm (dotted line). These measurements were performed using a sensor

TABLE I. Summary of different size defect detection measurement carried out on sample II. Detection is positive if a change in magnitude of thermal conductivity is observed.

Sensor radius (mm)	Defect cross section (cm ²)	Defect detection
9.868	3.14	Positive
9.868	0.79	Positive
9.868	0.2	Negative
3.18	0.2	Positive
9.868	0.03	Negative
3.189	0.03	Negative
2.001	0.03	Noisy data
0.526	0.03	Out of range

of radius 9.868 mm. In order to further investigate the effect of these defects, measurements are carried out using smaller radius sensor (3.18 mm) which resulted a detection for the 5 mm diameter defect, fig. 4 inset. Inset in fig. 4 shows the detection of the defect with smaller radius which other wise is not possible.

In an effort to detect the smallest (2 mm diameter) defect, different radius sensors were used. Yet detection of the smallest defect is still not possible. This is due to the short working distance for smaller sensors, as a reliable measurement depth is limited to the sensor diameter and bigger sensors are too big to see this defect. The detection measurement performed on sample II is summarized in the table I.

In addition to the radius of the sensor in relation to the defect cross section area, as demonstrated in table I, distance from the sensor affects the ability of the method to detect inhomogeneity. This is clearly demonstrated in fig. 5. The three curves in fig. 5 are obtained from similar defect located at different location, sample III, fig. 1(c). The figure compares the effect of cylindrical defects located at 2.5, 3.5 and 4.5 mm away from the sensor. The sensitivity of detection decrease as the distance from the sensor increases.

Similarly, the method's capability to pin point a hidden defect in the structure was tested. This was achieved by 3D printing of a material with a void region left inside, sample IV. Fig. 6 shows how thermal conductivity decreases as the thermal wave reaches the void region and eventually it rises again.

Similar to the previous figures, change in value of thermal conductivity along the depth indicates the presence of defect in the medium.

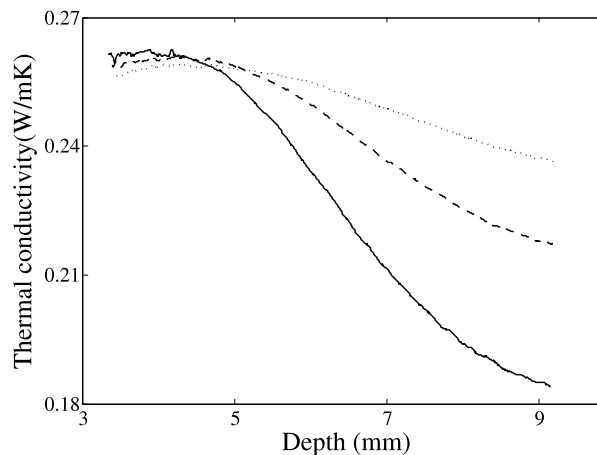


FIG. 7. Thermal conductivity measurements of a defect at different positions relative to the sensor.

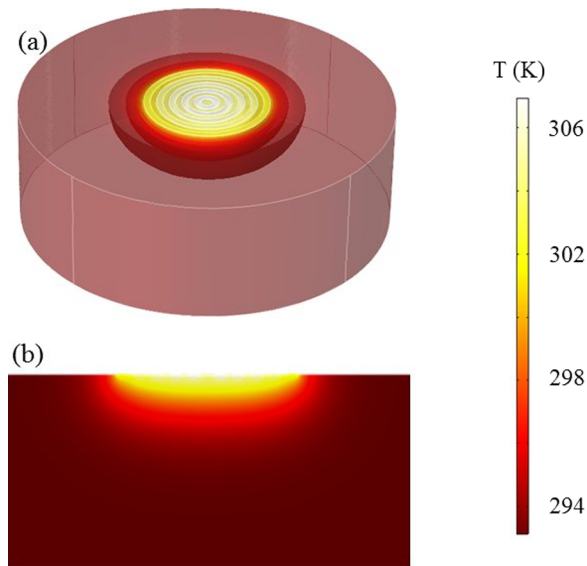


FIG. 8. (a) 3D temperature distribution in the material. Isothermal layers are represented by curved surface. (b) 2D cross-sectional view of temperature distribution along central axis.

In all of the above measurements (fig. 4 - 6), the center of the sensor and the defect were kept on a perpendicular line. The effect of misaligning the center of the defect from the sensor has also been investigated, fig. 7. Solid line: The center of the sensor is matched with the center of the defect, full area of the defect is covered with the sensor. Dashed line: The sensor center is positioned on the edge of the defect. In this case, less than half the area is covered by the sensor. dotted line: The sensor center is placed outside of the defect surface. The overlap area is less than quarter of the whole area .

Parallel to the previous results, the sensitivity decrease as the misalignment increases. Here, the idea is to see the effects of sensor location with respect to the fixed defect position. A sensor with radius of 9.868 mm on 20 mm diameter defect is used for fig. 7.

The detection mechanism is further investigated computationally, but it is important to note that our simulation, at this stage, does not provide thermal conductivity as it would be required if we were to directly compare experiment with simulation. Doing so requires simulation of the standard hot disk method and a detail study of the hot disk sensor which is the scope of an on-going project. The simulation rather provides time evolution of the sensor temperature and temperature profile of the material. This is justified by the fact that the present study mainly aims at demonstrating the possibility of nondestructive testing using thermal depth profiling.

B. Numerical Simulation

Two simulation models are included.

The first model is a cylindrical polymer (PDMS, Polydimethylsiloxane) material subjected to concentric heat source with and without an introduction of a PVC polymer as defect. The homogeneous PDMS cylindrical model has a radius of 15 mm and a height of 10 mm, fig. 8, whereas the defect PVC has a radius of 5 mm and height of 6 mm. This model demonstrates the basic principle of a transient method. It also shows the 3D spread of heat into the material and thus provides the temperature distribution of the sample, fig. 9.

The second model represents experimental sample II (a PVC polymer with four cylindrical voids) as displayed in fig. 2. This model compares the effect of defect size on the transient curve, fig. 10.

The simulated heat flow from a nickel heat source demonstrates the 3D spread of heat into the material. The temperature profile of the material after 40 seconds of constant heat is shown in fig. 8. 3D and 2D temperature profile of the sample in fig. 8(a) and 8(b) show temperature variations from

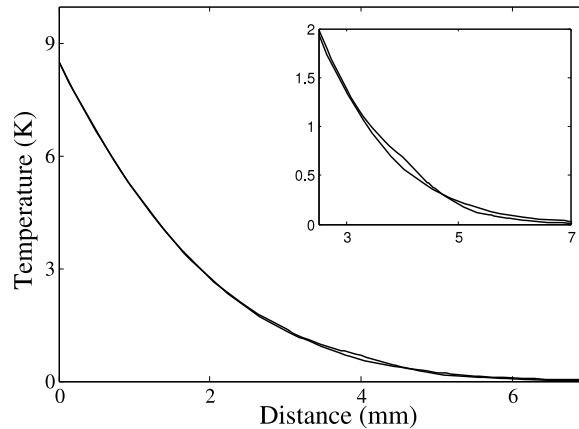


FIG. 9. Temperature profile of the material along the structure depth at $t=40$ seconds. The smooth curve is obtained from a homogeneous PDMS whereas the curve with anomalies has a PVC starting from 4 mm depth. Inset: shows the magnified view around the defect location.

maximum value of 306 K at the wires to initial temperature values at the opposite boundary of the sample.

The temperature profile of the sample can also be displayed by considering its distribution along a central axis. Fig. 9 shows a comparison of a homogeneous PDMS with and without an introduction of a PVC polymer as a defect, the first model. Generally the temperature drops as one goes from the surface in contact with the heat source to the rear end. The smooth curve represents the homogeneous PDMS, whereas the curve with the anomalies is obtained when PVC is present.

In numerical simulation, we use the change on the temperature of the sensor to discriminate between homogeneous and inhomogeneous materials. In fig. 10, the simulated transient curves acquired from the structure depicted in fig. 2 are presented. The sensor is placed perpendicular to each void. In fig. 10, the solid line is obtained when the sensor is placed perpendicular to largest void (cross sectional area of 3.14 cm^2). The dashed line is from the second largest void (cross sectional area of 0.79 cm^2) whereas the dot - dashed line and dotted line are from the defect of cross sectional area of 0.2 and 0.03 cm^2 respectively. This shows larger change in temperature for bigger defects. The difference between the various curves are better seen in the inset, when the temperature derivative is considered. Similar to the experimental result (table I), detection is possible for the two biggest defects, however, for the third defect, unlike the experiment, a slight change in temperature is observed in the simulation. The maximum temperature rise in each case is shown in table II.

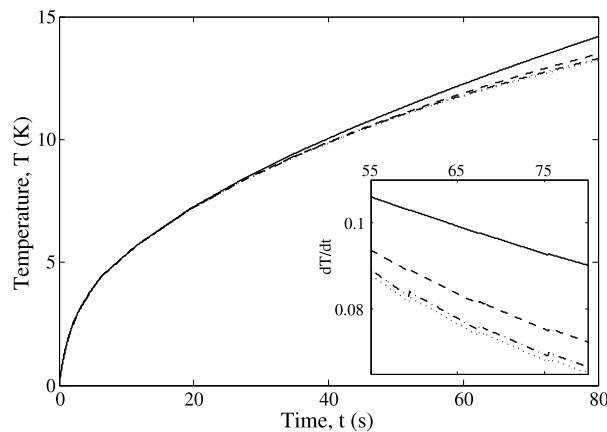


FIG. 10. Temperature evolution of the sensor placed on PVC polymer with four different size voids. Simulation result from fig. 2. Inset: Derivative of the temperature plotted against time.

TABLE II. Maximum temperature rise on the sensor. Detection is positive if the maximum temperature rise with and without the defect are different. Maximum temperature rise without a defect is 13.37 K. 10 mm radius sensor is used.

Defect radius (mm)	Maximum rise in temperature (K)	Defect detection
10	14.32 (solid line)	Positive
5	13.63 (dashed line)	Positive
2.5	13.43 (dot-dashed)	Positive
1	13.37(dotted line)	Negative

TABLE III. Maximum temperature recorded for different sensor position after 80 seconds. The sensor shows maximum temperature when the center of the sensor is aligned with the center of the defect (Center-to-center position, the perpendicular distance is zero).

Perpendicular distance (mm)	Maximum simulated temperature (K)
0	309.28
5	309.2
10	309.05
15	308.92
20	308.87

The effect of misalignment between the sensor and the defect is also demonstrated in the numerical simulation by shifting the sensor on the surface by a half radius distance, i.e changing the perpendicular distance between the fixed defect center and the sensor center. A rectangular block of sample (PVC) with a cylindrical void is considered. The rectangle has a dimension of 60 X 80 X 8 mm³. The radius of the sensor and void is set to 10 mm. The change in temperature on the sensor is recorded for different perpendicular position of the sensor with respect to fixed defect. The maximum change in temperature is observed when the sensor and the defect are aligned center-to-center whereas the lowest is recorded for edge-to-edge alignment. Table III summarizes the maximum temperature observed on the sensor for different sensor positions. Similar experimental results are demonstrated in fig. 7.

VI. SUMMARY AND CONCLUSION

In an effort to extend the hot disk method to study inhomogeneous materials, a recent attempt was made in designing an approximating scheme to estimate thermal conductivity versus depth of the materials. However, the capability and limitation of the method in characterizing inhomogeneous materials and detail experimental and numerical studies were not addressed. Thus, here we addressed the above issues using experimental and numerical works. The experimental work includes 3D printed detail polymer samples with voids of different size and position in the matrix where each sample were designed to address a particular property of the method. Finite element simulation of three-dimensional heat flow in an inhomogeneous material using a surface heat source and surface temperature sensing were employed to reveal the limitation and possibility of defect detection using this method.

Given the fact that, this is an approximate method and requires an *a-priori*-knowledge of volumetric specific heat capacity of the material to be investigated, one has to use the results with caution, for instance it is rather advisable to use the method for investigating trend in thermal conductivity instead of using it to measure the absolute thermal conductivity of the material.

Based on the results obtained in this work the following main conclusions are drawn:

- The method can verify structural homogeneity in a sample.
- For appropriate size and location of the defect, the method is sensitive enough to monitor the presence of inhomogeneity in the sample.
- The size of the sensor, size and location of the defect determine the sensitivity of the detection.

- Numerical simulation provides the temperature evolution of the sensor from which a difference between homogeneous and inhomogeneous samples can be inferred.

ACKNOWLEDGMENTS

This work is supported by Chalmers University of Technology Area of Advance Materials Science.

- ¹ L. Cartz, *Nondestructive Testing* (Materials Park, OH: ASM International, 1995).
- ² M. R. Jones, A. Tezuka, and Y. Yamada, *J. Heat Transfer* **117**, 969 (1995).
- ³ H. Ermert, F. H. Dacol, R. L. Melcher, and T. Baumann, *Appl. Phys. Lett.* **44**, 1136 (1984).
- ⁴ A. Rosencwaig, *Science* **218**, 4569 (1982).
- ⁵ J. Opsal and A. Rosencwaig, *J. Appl. Phys.* **53**, 4240 (1982).
- ⁶ J. A. Siddiqui, V. Arora, R. Mulaveesala, and A. Muniyappa, *Experimental Mechanics* **55**, 1239 (2015).
- ⁷ Y. He, *Thermochimica Acta* **436**, 122 (2005).
- ⁸ J. J. Healy, J. J. de Groot, and J. Kestin, *Physica* **82C**, 392 (1976).
- ⁹ S. E. Gustafsson, *J. Phys. D: Appl. Phys.* **19**, 727 (1986).
- ¹⁰ T. Log and S. E. Gustafsson, *Fire and Materials* **19**, 43 (1995).
- ¹¹ S. E. Gustafsson, *Rev. Sci. Instrum.* **62**, 797 (1991).
- ¹² ISO22007-2, "Plastics - determination of thermal conductivity and thermal diffusivity - part 2: Transient plane heat source (hot disc) method," (2008).
- ¹³ A. Sizov, D. Cederkrantz, L. Salmi, A. Rosen, L. Jacobson, S. E. Gustafsson, and M. Gustavsson, *Rev. Sci. Instr.* **87**, 074901 (2016).
- ¹⁴ H. S. Carslaw and J. C. Jaeger, *Conduction of heat in solids*, 2nd ed. (Oxford: Oxford University Press, 1959).
- ¹⁵ V. Gerlich, K. Sulovska, and M. Zalesak, *Measurement* **46**, 2003 (2013).
- ¹⁶ W. P. Roger, *Multiphysics Modeling using COMSOL: A first principles approach* (Jones and Bartlett, 2011).
- ¹⁷ M. Streza, Y. Fedala, J. P. Roger, G. Tessier, and C. Boue, *Meas. Sci. Technol.* **24**, 045602 (2013).